Resonance scattering at third-order exceptional points

W D Heiss[1,2], G Wunner[3],

[1]Department of Physics, University of Stellenbosch, 7602 Matieland, South Africa
[2]National Institute for Theoretical Physics (NITheP), Western Cape, South Africa
[3]Institut für Theoretische Physik, Universität Stuttgart, Pfaffenwaldring 57, 70 569 Stuttgart, Germany

E-mail: dieter@physics.sun.za

Abstract. We analyze scattering cross sections at and near third-order exceptional points (EP3), i.e., points in physical parameter space where three energies and eigenfunctions coincide. At an EP3, the Green's function contains a pole of third order, in addition to poles of second and first order. We show that the interference of the three pole terms produces a rich variety of line shapes at the exceptional point and in its neighbourhood. This is demonstrated by extending previous work on two harmonic oscillators to a system of three driven coupled damped oscillators. We also discuss the similarities and the differences in the behaviour of the amplitudes in the classical problem and the scattering cross sections in the quantum mechanical problem at the EP3.

PACS numbers: 03.65.Nk, 46.40.Ff, 03.65.Vf, 31.15.-p,

Submitted to: *J. Phys. A: Math. Gen.*

1. Introduction

Specific spectral singularities, that is singularities of eigenvalues of operators, have been dubbed exceptional points (EP) by Kato in his textbook 1966 [1]. In physics we are usually interested in EPs of Hamilton operators. They are isolated points in an (at least) two-dimensional parameter space at which two or even more eigenvalues coalesce. A coalescence is not a degeneracy since the corresponding eigenvectors become aligned meaning that there is no higher dimensional eigenspace. This is of course not possible for hermitian Hamiltonians, but it occurs in open quantum systems, in parity-time symmetric systems [2], systems with loss and gain [3–6] and others. Usual degeneracies may nevertheless also occur in non-hermitian problems. The physical effects of exceptional points of second order (EP2) have been discussed extensively in the literature, we refer the reader to review articles, e. g. [7–9], and references quoted therein.

In recent years, the effects of exceptional points of higher order [10], in particular of third order (EP3s), have received increasing attention. For example, the chirality of EP3s was analyzed bei Heiss [11], the behaviour of eigenfunctions when encircling an EP3 was discussed by Demange and Graefe [12] and Ryu *et al.* [13], and EP3s were shown to also appear in theoretical studies of Bose-Einstein condensates [14] and the Bloch equations [15].

The present paper studies the effect of poles of higher order in the scattering function at the EP. Our analysis focuses upon scattering cross sections at and near third-order exceptional points (EP3). At an EP3, the Green's function has a pole of third order, in addition to poles of second and first order. We show that the interference of the three pole terms produces a rich variety of line shapes at the exceptional point and in its neighbourhood. This is demonstrated by extending previous work on two harmonic oscillators [16–19] to a system of three driven coupled damped oscillators. We discuss the similarities and point out at the EP3 the differences between the behaviour of the classical amplitudes and the scattering cross sections of the corresponding quantum mechanical problem.

2. The model

We consider three one-dimensional harmonic oscillators with masses m_1, m_2, m_3, unperturbed eigenfrequencies ω_1, ω_2, ω_3 and damping constants k_1, k_2, k_3 being coupled by springs with spring constants f_{12}, f_{13}, f_{23} and associated dampings g_{12}, g_{13}, g_{23}. The system is driven by an external force with fixed period ω at one of the three oscillators. It is an extension of the model discussed in [16, 19, 20]. For the reader's convenience, we briefly describe the model of three coupled classical oscillators in analogy with [19]. Denoting by $p_1, p_2, p_3, q_1, q_2, q_3$ the momenta and spatial coordinates of three point particles with different masses the equations of motion read for the driven system

$$\frac{\mathrm{d}}{\mathrm{d}t}\begin{pmatrix} p_1 \\ p_2 \\ p_3 \\ q_1 \\ q_2 \\ q_3 \end{pmatrix} = \mathcal{M}\begin{pmatrix} p_1 \\ p_2 \\ p_3 \\ q_1 \\ q_2 \\ q_3 \end{pmatrix} + \begin{pmatrix} c_1 \\ c_2 \\ c_3 \\ d_1 \\ d_2 \\ d_3 \end{pmatrix} \exp(-\mathrm{i}\omega t) \tag{1}$$

with

$$\mathcal{M} = \begin{pmatrix} -2g_{12}-2g_{13}-2k_1 & 2g_{12} & 2g_{13} & -f_{12}-f_{13}-\omega_1^2 & f_{12} & f_{13} \\ 2g_{12} & -2g_{12}-2g_{23}-2k_2 & 2g_{23} & f_{12} & -f_{12}-f_{23}-\omega_2^2 & f_{23} \\ 2g_{13} & 2g_{23} & -2g_{13}-2g_{23}-2k_3 & f_{13} & f_{23} & -f_{13}-f_{23}-\omega_3^2 \\ 1/m_1 & 0 & 0 & 0 & 0 & 0 \\ 0 & 1/m_2 & 0 & 0 & 0 & 0 \\ 0 & 0 & 1/m_3 & 0 & 0 & 0 \end{pmatrix}$$

and c_i, d_i denoting initial conditions for the classical problem; they are of no importance for the quantum mechanical treatment. Time-periodic solutions and resonances with real frequency ω are found by the roots of the characteristic polynomial of the matrix $\mathcal{M}$.

EP3s occur for complex values of ω where the characteristic polynomial of $\mathcal{M}$ as well as its first *and* the second derivatives vanish, i.e.

$$\det(\mathcal{M} + \mathrm{i}\omega) = 0, \ \frac{\mathrm{d}}{\mathrm{d}\omega}\det(\mathcal{M} + \mathrm{i}\omega) = 0, \ \frac{\mathrm{d}^2}{\mathrm{d}^2\omega}\det(\mathcal{M} + \mathrm{i}\omega) = 0. \quad (2)$$

These equations lead to 6 real-valued equations for the 17 real parameters

$$\omega_i, k_i, m_i, g_{ij}, f_{ij}, (i,j = 1,2,3), \Re(\omega), \Im(\omega),$$

$\Re(\omega)$ and $\Im(\omega)$ denoting the real and imaginary parts of ω, respectively. To reduce the number of free physical parameters we study the special case that the oscillators themselves are undamped, $k_1 = k_2 = k_3 = 0$, and that there is no coupling between oscillator 1 and 3, $f_{13} = g_{13} = 0$. Then we are left with the simpler matrix

$$M = \begin{pmatrix} -2g_{12} & 2g_{12} & 0 & -f_{12}-\omega_1^2 & f_{12} & 0 \\ 2g_{12} & -2g_{12}-2g_{23} & 2g_{23} & f_{12} & -f_{12}-f_{23}-\omega_2^2 & f_{23} \\ 0 & 2g_{23} & -2g_{23} & 0 & f_{23} & -f_{23}-\omega_3^2 \\ 1/m_1 & 0 & 0 & 0 & 0 & 0 \\ 0 & 1/m_2 & 0 & 0 & 0 & 0 \\ 0 & 0 & 1/m_3 & 0 & 0 & 0 \end{pmatrix}.$$

Equations (2) can be solved only numerically. With further values given for the oscillator frequencies and the masses, complex solutions for the remaining parameters are found in general. It should be noted that complex solutions of (2) always exist. The challenge is to find solutions being physically acceptable, that is the spring and damping constants must be real and positive, i.e. $f_{ij} > 0$, $g_{ij} > 0$, and the width should obey $\Im(\omega) < 0$; we focus on positive frequencies, i.e. $\Re(\omega) > 0$. In addition, solutions should not only be physically acceptable but also of physical interest: for instance, an EP3 lying far away from the real axis cannot yield much structure on the real axis, in other words, a small width is desirable.

Having set the values for ω_i and m_i, $i = 1, \ldots, 3$ we numerically seek EP3s. Our interest is focused upon the 4-th quadrant in the complex ω-plane where usually a few solutions occur. For given $f_{12} > 0$ and $f_{23} > 0$ we obtain solutions with complex values for g_{12}, g_{23} and ω. Of those we concentrate upon a particular solution that comes closest to the constraints as imposed above. By re-adjusting the values for $f_{12} > 0$ and $f_{23} > 0$ we obtain in certain cases solutions that satisfy the constraints. For the model considered it appears that acceptable solutions (e.g. small width) could not be found for all three masses being equal. In fact, even when two masses are equal,

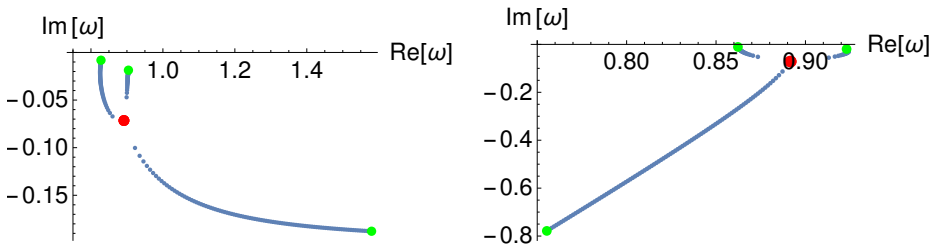

Figure 1. Left: Eigenvalue trajectories emerging from the EP3 (red dot) when f_{12} is varied from $f_{EP} = 0.021$ to $f_{12} = 0.92$ (green dots). Right: Trajectories when g_{12} is varied from $g_{EP} = 0.098$ to $g_{12} = 0.25$. Notice the different scales: the red dot has the same coordinates. Choice of parameters see Sec.3.

the width still turned out to be unsuitably large. We cannot claim to have searched the whole set of parameters. In view of our interest being directed to three-channel scattering problems a wider search may be sensible and necessary once a specific experimental setting is realised.

The reduction in the vicinity of the EP3 from the six- to a three-dimensional problem follows the lines similar to those applied in [22]. In Fig. 1 we display trajectories of eigenvalues in the ω-plane. For the region considered they coincide perfectly with those from the original six-dimensional problem. Note that the position of the EP3 is independent of the initial conditions and so are the eigenvalues (trajectories in Fig. 1). We mention that any two of the three different eigenvalues are connected at an EP2 but these are not drawn as they occur for complex values of the coupling parameters. We recall that the eigenvalues displayed in Fig. 1 give rise to resonances of the classical amplitudes of the oscillators while they are as well the pole positions, i.e. scattering resonances, of the Green's function used for the three-channel scattering problem. Only at the EP3, where the trajectories coalesce, the scattering problem will be different from the classical oscillators owing to the all important interference of the third, second and first order pole terms of the Green's function at the EP3. These facts will be discussed in the following Section.

3. Results

Using the parameters $m_1 = 1, m_2 = 3, m_3 = 4$ and $\omega_1 = 1, \omega_2 = 1.4, \omega_3 = 1.7$ we obtain an acceptable EP3 at $\omega_{EP3} = 0.89 - \mathrm{i}\,0.071$ for the couplings $f_{12} = 0.021, f_{23} = 0.23, g_{12} = 0.098, g_{23} = 0.0095$ (actually the values are obtained at much higher precision). If one intends to study the vicinity of the EP3, one has to realise an important characteristic of the EP3: owing to the higher number of parameters there is a multitude of possibilities to unfold the three eigenvalues when moving away from the EP3. The trajectories displayed in Fig. 1 using the two different parameters f_{12} and g_{12} are manifestly different. In the following we denote by H the three dimensional matrix obtained by reducing the six dimensional matrix M [22] (see also [19], appendix) . It depends on all coupling parameters. To study the dependence on a specific parameter we denote by x the selected coupling parameter, and by M_0 we denote the matrix where that specific parameter is set equal to zero in H while all other parameters assume their values at the EP3. Formally, the decomposition

$$H = M_0 + xM_1,$$

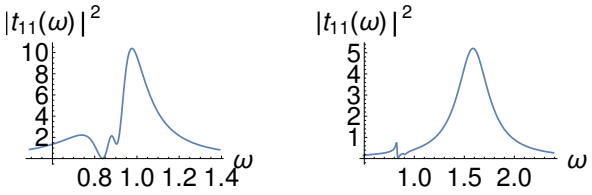

Figure 2. Cross section $|t_{11}(\omega)|^2$ for $f_{12} = 0.021$ (the value at the EP3) and for $f_{12} = 0.92$

yields different three-dimensional matrices M_0 and M_1 for different choices of the parameter x as long as H is taken at an EP3. As a consequence, while the Green's function has at the EP3 the form [21]

$$(H - E_{EP3})^{-1} = \frac{I}{\omega - E_{EP3}} + \frac{H - IE_{EP3}}{(\omega - E_{EP3})^2} + \frac{(H - IE_{EP3})^2}{(\omega - E_{EP3})^3}$$

with I being the identity matrix, the scattering matrix element

$$t_{i,k}(\omega) = (M_1(H - E_{EP3})^{-1}M_1)_{i,k} + (M_1)_{i,k}$$

will also be different for different choices of x. Recall that, for the cross section, $|M_1(H - E_{EP3})^{-1}M_1|^2$ has to be considered giving rise to interference terms from the poles of different order (for simplicity the energy independent part M_1 is left out as it is insignificant.) In other words the cross section at the EP3 is different depending on the choice of x. Note that this feature renders an experimental realisation of an EP3 with a rich and challenging structure.

We here present three distinct choices. Results displayed refer to a single channel cross section of the quantum mechanical three channel scattering of three coupled oscillators; the other direct channels look the same up to a factor. In Fig. 2 we illustrate results using $x = f_{12}$.

Similar to the case for an EP2 we recall that the various peaks at the left hand figure cannot be associated with a particular resonance pole. Also similar to the case of the EP2 is the zero of the scattering amplitude due to interference; the zero disappears and becomes a minimum when one or more of the damping constants k_i are switched on. At the EP3, where the scattering amplitude has poles of different order at the same position, the pattern is essentially generated by the structure of the various interference terms. The all important role of the interference terms is illustrated in Fig. 3. Only the sum of the interference terms and of the pole terms of different order yields the final pattern as illustrated in Fig. 2. In contrast, moving away from the EP3, the distinct peak at the right hand illustration is clearly caused by a traditional resonance pole term; it is the pole related to the green dot on the right of the left hand panel of Fig. 1. The smaller structure of the right hand panel of Fig. 2 is still due to the combined effect of the interference terms being, however, much smaller and the two poles with smaller width (see left hand panel of Fig. 1). This is illustrated on the bottom row of Fig. 3. The interference shows its effect only at the pole terms with small width.

Let us contrast these results with those obtained by the choice $x = g_{12}$.

It is evident that the displays of Fig. 4 are distinctly different from those in Fig. 2, albeit there is a qualitative similarity, especially on the respective left hand panels (at

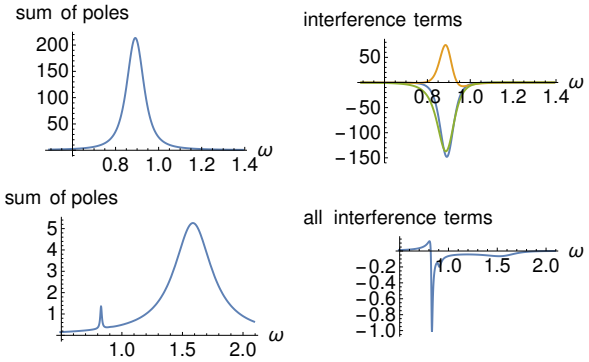

Figure 3. Individual contributions of the pole and interference terms to the cross sections shown in Fig. (2). Top left: sum only of the pole terms of third, second and first order, all at the same position. Top right: the three individual interference terms. Bottom left: contributions of the individual first order poles; the residue of one of the poles with small width is very small. Bottom right: sum of interference terms.

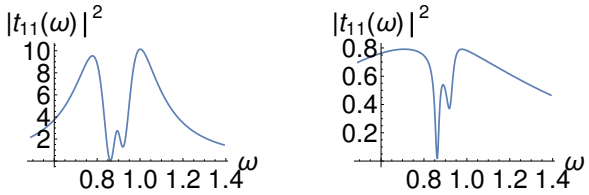

Figure 4. Cross section $|t_{11}(\omega)|^2$ for $g_{12} = 0.098$ (the value at the EP3) and for $g_{12} = 0.25$

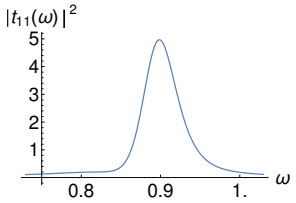

Figure 5. Cross section $|t_{11}(\omega)|^2$ choosing $x = f_{23}$, all parameters at the EP3.

the EP3). Further away from the EP3 (right hand panel) the gross pattern in Fig. 4 is dominated by the contribution from a distant resonance pole with a large width ($\omega_{\rm res} = 0.75 - {\rm i}\,0.8$, see Fig. 1 right hand panel) while the substructure is caused by the interference terms and the other two poles with small widths.

To underline the variety of possible structures we display in Fig. 5 the result of choosing $x = f_{23}$. The illustration presents a situation where the interference terms are of minor importance. Yet they produce an asymmetry for the sum of the three pole terms at the EP3. It is obvious that the peak has not the shape of a Lorentzian. We mention that the patterns remain qualitatively unchanged when all the masses are multiplied by the factor 2. Yet, the EP3 then occurs for $\omega_{EP3} = 0.63 - {\rm i}\,0.051$.

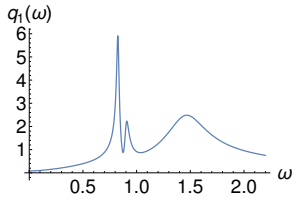

Figure 6. Amplitude of the first oscillator *versus* exciting frequency.

The interference terms dominate the whole pattern at the EP3. It is as such a typical quantum mechanical or wave mechanical problem that has no analogy for the three classical oscillators. However, further away from the spectral singularity, where each individual pole of the three poles can produce a resonance, it is of some interest to compare typical classical amplitudes with the corresponding wave scattering phenomena. In Fig. 6 we illustrate the amplitude of the first oscillator (smallest mass) using the initial condition $q_1 = 1$, $q_2 = q_3 = 0$ with all initial momenta equal to zero. The three resonances (green points on left hand panel of Fig. 1) are clearly discernible.

The other oscillators show similar patterns owing to the mutual coupling. However, at the EP3 the classical amplitudes have little or no structure in contrast to the pronounced interference patterns for the scattering amplitudes.

4. Summary and Conclusion

The dominance of interference upon scattering at an EP has been demonstrated for an EP2 in [19, 20]. There it has been found that two distinct peaks at the EP2 cannot be associated with two individual resonance poles but are brought about by the interference of poles of different order at the same position. The present study has clearly shown the by far richer structure of basically the same phenomenon for scattering using parameters giving rise to an EP3 or its vicinity. In fact, at the EP3 three peaks can occur owing to a similar mechanism, i.e. by the interference of three poles of different order at the same position. Furthermore, while the position of the EP3 is a fixed point in parameter space the sprouting out of the three levels under parameter variation depends on the particular parameter chosen. Moreover, for the cross section the precise pattern at the EP3 is different depending on the particular approach of the EP3 within the high dimensional parameter space. In principle, this could be expected as an EP3 can also be seen as the confluence of two EP2s that share a Riemann sheet in the complex energy plane. And it is here where the increased complexity can be visualised. Depending on the choice of the specific parameter that is varied to make the three eigenvalues sprout into three different directions, the respective two EP2s connecting two different pairs of the three levels are themselves arranged and connected differently depending on the parameter choice. Even though the two EP2 are usually not amenable physically - they have non-real coupling constants -, yet it is this mathematical structure that explains the different patterns at the EP3 and its vicinity for variations of different parameters.

We are aware that there are much simpler, but non-generic cases of EP3 or even higher order EPs (see e.g. [12]). While these cases have their merit such as, for instance, in the associated study of subclasses of EPs of lower order, our study reveals a rich structure that can occur already for a third order EP. Recall that we have

already reduced the actual number of parameters by pre-setting to zero the damping and some coupling constants. An even more detailed study is indicated when an actual experimental situation is at hand.

To dissolve such rich and delicate structure in the laboratory means of course a considerable challenge for experimentation. As there are a number of cases for the occurrence of an EP3 discussed in the literature (see Introduction), we feel there is a good chance to show that these structures are in fact a physical reality. One realisation could be measuring transmission profiles through three coupled wave guides with gain and loss as suggested in [12]. Another possibility could be an extension of a microwave cavity experiment with three partitions of the cavity instead of the two. After all, it was about 15 years ago when the first encircling of an EP2 was successfully achieved for the two partitions [23]. A particular experimental study seems to be under way using three different coupled cavities [24].

Acknowledgement

WDH and GW gratefully acknowledge the support from the National Institute for Theoretical Physics (NITheP), Western Cape, South Africa. GW expresses his gratitude to the Department of Physics of the University of Stellenbosch where this work was carried out.

References

[1] T. Kato. *Perturbation theory for linear operators*. Springer, Berlin, 1966.
[2] C. M. Bender and S. Boettcher. Real spectra in non-Hermitian Hamiltonians having $\mathcal{PT}$ symmetry. *Phys. Rev. Lett.*, 80:5243, 1998.
[3] A. Guo, G. J. Salamo, D. Duchesne, R. Morandotti, M. Volatier-Ravat, V. Aimez, G. A. Siviloglou, and D. N. Christodoulides. Observation of $\mathcal{PT}$-symmetry breaking in complex optical potentials. *Phys. Rev. Lett.*, 103:093902, 2009.
[4] Ch. E. Rüter, K. G. Makris, R. El-Ganainy, D. N. Christodoulides, M. Segev, and D. Kip. Observation of parity-time symmetry in optics. *Nat. Phys.*, 6:192, 2010.
[5] A. Regensburger, Ch. Bersch, M.-A. Miri, G. Onishchukov, D. N. Christodoulides, and U. Peschel. Parity-time synthetic photonic lattices. *Nature*, 488:167, 2012.
[6] D. Dast, D. Haag, H. Cartarius, G. Wunner, R. Eichler, and J. Main. A Bose-Einstein condensate in a $\mathcal{PT}$ symmetric double well. *Fortschritte der Physik*, 61:124–139, 2013.
[7] N. Moiseyev. *Non-Hermitian Quantum Mechanics*. Cambridge University Press, Cambridge, 2011.
[8] I. Rotter. A non-Hermitian Hamilton operator and the physics of open quantum systems. *J. Phys. A*, 42:153001, 2009.
[9] W. D. Heiss. The physics of exceptional points. *J. Phys. A*, 45:444016, 2012.
[10] E.-M. Graefe, U. Günther, H. J. Korsch, and A. E. Niederle. A non-Hermitian $\mathcal{PT}$ symmetric Bose-Hubbard model: eigenvalue rings from unfolding higher-order exceptional points. *J. Phys. A*, 41:255206, 2008.
[11] W. D. Heiss. Chirality of wavefunctions for three coalescing levels. *J. Phys. A*, 41:244010, 2008.
[12] G. Demange and E.-M. Graefe. Signatures of three coalescing eigenfunctions. *J. Phys. A*, 45:025303, 2012.
[13] J.-W. Ryu, S.-Y. Lee, and S. W Kim. Analysis of multiple exceptional points related to three interacting eigenmodes in a non-hermitian hamiltonian. *Phys. Rev A*, 85:042101, 2012.
[14] R. Gutöhrlein, J. Main, H. Cartarius, and G. Wunner. Bifurcations and exceptional points in dipolar Bose-Einstein condensates. *J. Phys. A*, 46:305001, 2013.
[15] M. Am-Shallem, R. Kosloff, and N. Moiseyev. Exceptional points for parameter estimation in open quantum systems: Analysis of the Bloch equations. arXiv:1406.6364v2.
[16] W. D. Heiss. Exceptional points of non-Hermitian operators. *J. Phys. A*, 37:2455, 2004.
[17] Y. S. Joe, A. M. Satanin, and Ch. S. Kim. Classical analogy of Fano resonances. *Phys. Scripta*, 74:259, 2006.

[18] A. E. Miroshnichenko, S. Flach, and Y. S. Kivshar. Fano resonances in nanoscale structures. *Rev. Mod. Phys.*, 82:2257, 2010.
[19] W. D. Heiss and G. Wunner. Fano-Feshbach resonances in two-channel scattering around exceptional points. *Eur. Phys. J. D*, 68:284, 2014.
[20] L. Schwarz, H. Cartarius, G. Wunner, W. D. Heiss, and J. Main. Fano resonances in scattering: An alternative perspective. arXiv:1503.08707v2.
[21] W. D. Heiss. Green's functions at exceptional points. J. Theor. Phys., in press, DOI:10.1007/s10773-014-2428-7.
[22] W. D. Heiss and H. L. Harney The chirality of exceptional points *Eur. Phys. J. D*, 17:149, 2014.
[23] C. Dembowski, H.-D. Gräf, H. L. Harney, A. Heine, W. D. Heiss, H. Rehfeld, and A. Richter. Experimental observation of the topological structure of exceptional points. *Phys. Rev. Lett.*, 86:787–790, Jan 2001.
[24] Ulrich Kuhl, private communication